One-pot Preparation of Porphyrin-Sensitized ZIF-8 as a Visible Light Photocatalyst

Xiaodong Zhang[1] , Yuhan Duan[1] , Qian Duan[1,*]

[1] School of Materials Science and Engineering, Changchun University of Science and Technology, Changchun, 130022, China

Abstract: Tetraaminoporphyrin (TAPP) sensitized ZIF-8 was successfully prepared by one-pot method as an efficient visible light photocatalyst. The prepared photocatalyst TAPP/ZIF-8 was characterized by XRD and SEM. The combination of TAPP and ZIF-8 enhances the absorption of visible light, effectively improves the electron-hole separation, and improves the photocatalytic activity under visible light. In the photocatalytic experiment, TAPP/ZIF-8 showed good photocatalytic performance for the removal of Rhodamine B (RhB) under visible light. Therefore, our work provides an efficient green photocatalyst for water treatment.

1.Introduction

In recent years, due to the rapid development of textile, automobile, electronic products, medicine and other industries, a large number of harmful substances are inevitably produced in the production process, especially harmful substances entering rivers, farmland, air and other areas closely related to life, which not only cause serious harm to the environment, but also pose a great threat to human health [1-3]. The dye molecules released during the production process are considered to be one of the most common sources of water pollution. Due to the potential carcinogenic threat, there is an urgent need for efficient and convenient methods to remove pollutants in water. As we all know, solar energy is an inexhaustible clean energy. Semiconductor photocatalysis is considered to be a green wastewater treatment method because solar energy can be used to degrade harmful pollutants. In the past few decades, it has been widely studied [4-5].

As the most popular hybrid material in recent years, metal-organic frameworks (MOFs) have been widely used in photocatalytic CO_2 reduction, photocatalytic water splitting and photocatalytic organic pollutants due to their unique porous structure and physicochemical properties. These applications are of great value to environmental protection and resource utilization. It also makes MOFs materials considered to be one of the most promising materials [6]. As a catalyst, the mechanism of MOFs in the catalytic process is different from that of traditional catalysts. Due to the unique surface area and porous structure of MOFs, CO_2 or polluted water is first adsorbed around MOFs, and these CO_2 or polluted water can enter the peculiar channels and pores of MOFs and interact with inorganic ions or organic ligands. Then under the conditions of light, heat, ultrasound, etc., the metal ions in MOFs are excited and converted into a high-energy state, which will react with the substances adsorbed on the surface or in the pore size to achieve the purpose of photocatalytic redox [7].

ZIF-8 is a porous nanomaterial assembled by metal clusters and organic molecules. Due to its considerable specific surface area and pore volume, as well as very stable chemical and physical properties, it has been widely used in photocatalysis, adsorption, energy storage and so on. A large number of studies have shown that ZIF-8 has shown very good performance in the degradation and adsorption of pollutants such as organic dyes. However, it only has ultraviolet light response, so it can only absorb ultraviolet light, so the utilization rate of solar energy is relatively low, which limits its further application in the field of photocatalysis [8].

There are a large number of conjugated double bonds and heterocyclic structures in the molecular structure of porphyrin, which makes it have a wide range of absorption spectra [9]. Porphyrin can absorb the spectrum of visible light and even near infrared region, and can effectively use solar energy. And their chemical structure gives them high stability, strong biocompatibility and reusability. Therefore, porphyrins and their derivatives with strong light responsiveness have been used as sensitizers for many semiconductor catalysts [10-11].

In this work, TCPP/ZIF-8 was prepared by a simple one-pot synthesis, and the synergistic photocatalytic performance of TCPP/ZIF-8 was evaluated using the photocatalytic degradation of Rhodamine B (RhB) dye as a pollutant model. Due to its ingenious experimental ideas, the obtained TAPP-sensitized ZIF-8 exhibits excellent visible light catalytic activity. Most importantly, this study provides a new way for porphyrin and MOFs composite photocatalysts in water pollution control.

* Corresponding author: duanqian88@hotmail.com.

2. Experimental

2.1. Materials

Zinc acetate dihydrate, 2-methylimidazole and 4-Nitrobenzaldehyde from Aladdin Industrial Corporation, nitrobenzene, lactic acid, pyrrole, $Na_2S·9H_2O$, NH_4Cl, *N*, *N*-Dimethylformamide (DMF), methanol and dichloromethane were provided by Macklin Biochemical Co., Ltd.

2.2 Synthesis of TAPP

Tetranitroporphyrin (TAPP) was synthesized by the Adler method. The experimental synthesis route is shown in Fig. 1. The specific process is as follows: 4-Nitrobenzaldehyde (4.0 g, 26.5 mmol) was added to a flask (100 mL), dissolved with nitrobenzene (25 mL), and lactic acid (15 mL) was added. Under the condition of solvent reflux at 140 °C, pyrrole (1.83 mL, 26.5 mmol) diluted with 20 mL of nitrobenzene was dropped, then it was heated to 140 °C for 2 h. After that, the temperature was reduced to 60 °C and 15 mL methanol was added to continue stirring for 30 min. After the reaction, the mixture was placed overnight, filtered by vacuum, the filter cake was collected and washed with ethanol. The purple solid (1.2 g) was obtained by drying in a vacuum drying oven for 12 h. The obtained TNPP was reduced by $Na_2S·9H_2O$ to obtain TNPP. The specific process was as follows: TNPP (0.5 g, 0.6 mmol), $Na_2S·9H_2O$ (5.2 g, 21.6 mmol) and NH_4Cl (160 mg, 3 mmol) were added to single-mouth flask (100 mL), it was dissolved in DMF (50 mL) and reacted at 70 °C for 12 h. The resulting samples were then poured into ice water (500 mL) for sedimentation. After filtration, drying. The dried solid was subjected to Soxhlet extraction. The solvent was dichloromethane. The liquid product was collected and the solvent was removed by rotary evaporation to obtain a purple powder sample. Then it was separated and purified by column chromatography. The eluent was methanol: dichloromethane = 1: 70 (V/V). Remove solvent, vacuum drying purple powder was 0.316 g, and the yield was 75 %. FT-IR (KBr pellet) ν:3437, 3344, 3025, 1614, 1512, 1468, 1285, 966, 801, 735 cm^{-1}. 1H NMR (500 MHz, DMSO-d_6) δ (ppm): 8.89 (s, 8H), 7.95–7.79 (m, 8H), 7.06–6.95 (m, 8H), 5.60 (s, 8H), -2.74 (s, 2H).

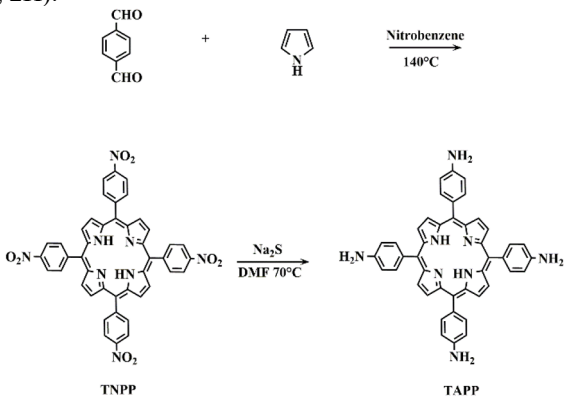

Fig. 1. Synthesis route of TAPP

2.3 Synthesis of TAPP/ZIF-8

Zinc acetate dihydrate (0.14 g) and 2-methylimidazole (2.27 g) were added to 5 mL methanol, respectively, and stirred for 60 min to form solution a and solution b. Then the above two solutions were mixed and TAPP (100 mg) was added, and the solution c was obtained by mechanical stirring for 60 min at room temperature. The solution c was added to the autoclave and hydrothermally synthesized at 120 °C for 12 h. After the temperature of the vacuum drying oven is slowly reduced to room temperature, the product is collected by centrifugation and drying. The centrifugation process uses a large amount of methanol and ethanol for multiple cleaning.

2.4 Photocatalytic experiments

The photocatalytic performance of the samples was evaluated by the removal rate of RhB. The experimental simulated light source was Xe lamp (300 W) with a filter with λ>400 nm. The mass of the photocatalyst was 10 mg, the concentration of the simulated pollutant RhB solution was 1.0×10^{-5} mol/L, and the solution volume was 40 mL. Before using Xe lamp for illumination, in order to ensure the dispersion stirring, we added magnetons and stirred them, and carried out dark adsorption for 60 min under dark conditions to ensure adsorption and desorption equilibrium. The concentration of simulated pollutant RhB was detected by ultraviolet-visible spectrophotometer at 554 nm at different time points.

3. Results and Discussion

3.1. Synthesis and Characterization

The crystal phases of ZIF-8 and TAPP/ ZIF-8 were characterized by XRD, and the results were shown in Fig. 2. The XRD pattern of ZIF-8 shows a high intensity diffraction peak. The diffraction peaks at 10.6 °, 12.9 °, 14.9 °, 16.6 ° and 18.2 ° correspond to the (311), (400), (422), (511) and (440) crystal planes of ZIF-8, respectively. For the XRD pattern of TAPP/ZIF-8, we found that the addition of TAPP did not change the position of any characteristic diffraction peak of ZIF-8, but we were surprised to find that the characteristic peak of TAPP/ZIF-8 obtained by one-pot method after doping TAPP was more obvious, showing a more stable crystal characteristic peak. The possible reason is that during the preparation of TAPP/ZIF-8 by one-pot method, two ligands TAPP and dimethylimidazole formed a competitive relationship during the growth of ZIF-8 crystal, resulting in more complete coordination with zinc ions. As a result, the prepared ZIF-8 structure is more stable. The above results show that the ZIF-8 obtained by one-pot method has good crystallinity, and it is also proved that the introduction of TAPP will not affect the crystal structure of ZIF-8 in the process of preparing TAPP/ZIF-8 by one-pot method.

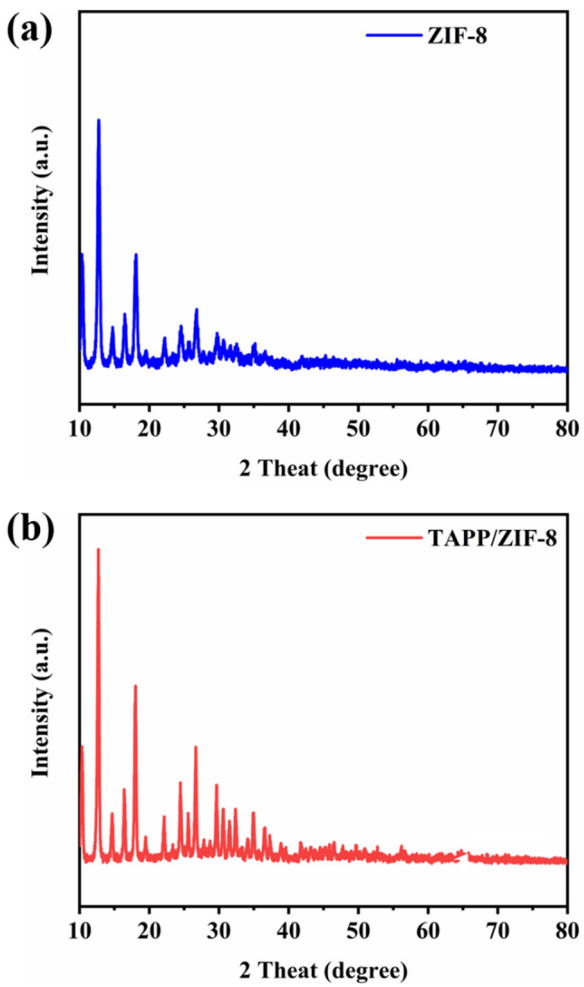

Fig. 2. XRD patterns of ZIF-8 (a) and TAPP/ZIF-8 (b).

The microstructure of ZIF-8 and TAPP/ZIF-8 was studied by SEM. It can be seen from Fig. 3(a) that the prepared ZIF-8s have a diameter of about 1μm, a smooth surface, and a rhombic dodecahedron shape. Fig. 3(b) shown that the morphology of TAPP/ZIF-8 prepared by one-pot method did not change significantly after adding TAPP, and the size was also consistent with that of ZIF-8 prepared without adding TAPP, it shows that the microstructure of ZIF-8 does not change after doping TAPP. In addition, the illustrations in the upper right corner of Fig. 3(a) and Fig. 3(b) are physical pictures of ZIF-8 and TAPP/ZIF-8. It can be seen that ZIF-8 without TAPP is white powder. The color is light green after the addition of TAPP, indicating that the addition of TAPP changes the color of ZIF-8, which further proves the effective doping of TAPP.

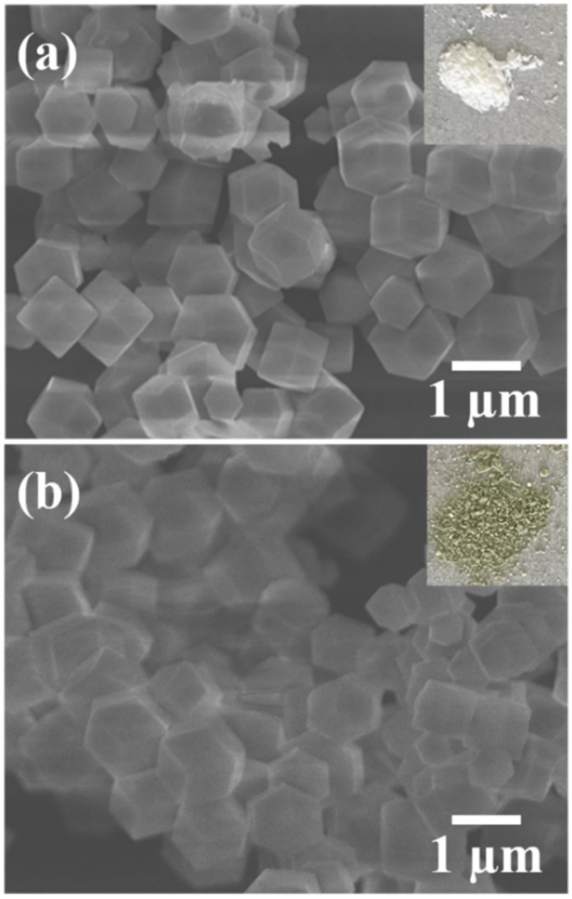

Fig. 3. SEM images of ZIF-8 (a) and TAPP/ZIF-8 (b), the illustration is the corresponding physical picture photo.

3.2. Photocatalytic activity

In order to demonstrate the advantages of doped TAPP/ZIF-8 prepared by one-pot method, we evaluated the photocatalytic performance of three different samples TAPP, ZIF-8 and TAPP/ZIF-8 by the degradation rate of RhB. From Fig 4, it can be seen that pure TAPP exhibits a lower adsorption rate and degradation rate for RhB due to its relatively low specific surface area and the recombination rate of photogenerated electron-hole pairs. As one of the most classic members of MOFs, ZIF-8 exhibits excellent adsorption performance for RhB., and the adsorption rate reached 38%. TAPP/ZIF-8 also showed excellent adsorption performance after doping TAPP, and the adsorption rate was 31%. The reason for the decrease may be that the doped TAPP occupies a part of the pore size and surface of ZIF-8, which affects the adsorption rate of RhB to a certain extent. In addition, since ZIF-8 only has ultraviolet light response ability, it also demonstrates a low degradation rate of RhB under visible light. TAPP/ZIF-8 can make full use of the visible light response after TAPP sensitization. As shown in Fig. 4, TAPP/ZIF-8 exhibits the best visible light photocatalytic performance, and the photocatalytic degradation efficiency of RhB is as high as 82 % within 120 min.

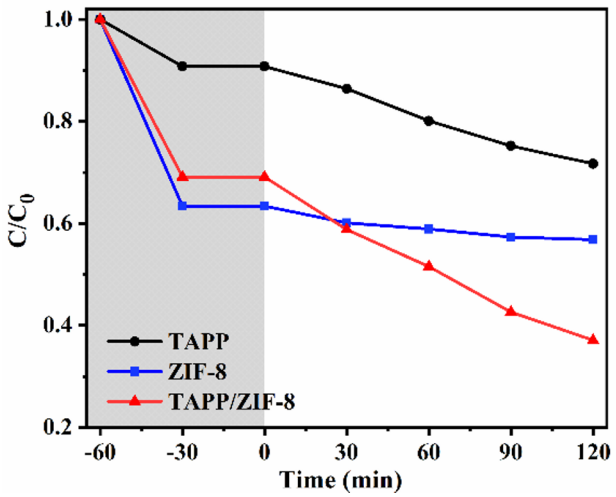

Fig. 4. Photocatalytic oxidation of RhB by TAPP, ZIF-8 and TAPP/ZIF-8 under visible light.

4. Conclusins

In summary, a novel green photocatalyst TAPP/ZIF-8 was prepared by a simple and convenient one-pot method. TAPP is effectively doped into the ZIF-8 structure, and the TAPP-sensitized ZIF-8 has a light response in the visible region. In addition, the heterojunction formed by the composite material may reduce the recombination rate of photogenerated electron-hole pairs in the catalyst, thereby enhancing the photocatalytic activity. Therefore, this study provides a useful method for the preparation of porphyrin and its derivatives with MOFs composites, making it an ideal photocatalyst for environmental governance, especially for sewage treatment.

Acknowledgements

This work was financially supported by the Jilin Science & Technology Department (grant number YDZJ202301ZYTS266); Jilin Province Association for Science and Technology (grant number QT202223).

References

1. J., Wen, H.J., Wang, Y., Li, X.G., Zheng, Integrating MoS_2 with S, P, N-codoped carbon nanofibers for efficient adsorption-photocatalytic degradation of dye, Ceram Int., 49 (2023) 5667-5675, https://doi.org/10.1016/j.ceramint.2022.11.247.
2. F.Y., Xu, J.J., Zhang, B.C., Zhu, J.G., Yu, J.S., Xu, $CuInS_2$ sensitized TiO_2 hybrid nanofibers for improved photocatalytic CO_2 reduction, Appl Catal B-Environ, 230 (2018) 194-202, https://doi.org/10.1016/j.apcatb.2018.02.042.
3. S., Afzal, W.A., Daoud, S.J., Langford, Visible-light self-cleaning cotton by metalloporphyrin-sensitized photocatalysis, Appl Surf Sci, 275 (2013) 36-42, http://dx.doi.org/10.1016/j.apsusc.2013.01.141.
4. J., Tian, Z.H., Zhao, A., Kumar, R.I., Boughton, H., Liu, Recent progress in design, synthesis, and applications of one-dimensional TiO_2 nanostructured surface heterostructures: a review, Chem Soc Rev, 43 (2014) 6920-6937, https://doi.org/10.1039/c4cs00180j.
5. H.Y., Wu, T.， Inaba, Z.M.， Wang, T., Endo, Photocatalytic TiO_2@CS-embedded cellulose nanofiber mixed matrix membrane, Appl Catal B-Environ, 276 (2020) 119111, https://doi.org/10.1016/j.apcatb.2020.119111.
6. H.L., Hou, L. Wang, F., Gao, G. D., Wei, B., Tang, W. Y., Yang, T., Wu, A General Strategy for Fabricating Thoroughly Mesoporous Nanofibers, J Am Chem Soc, 136, (2014) 16716–16719, https://doi.org/10.1021/ja508840c.
7. Y., Hong, B. L., Wang, S. S., Hu, S., Lu, Q., Wu, M. M., Fu, C. Z., Gu, Y. Z., Wang, Preparation and photocatalytic performance of Zn_2SnO_4/ZIF-8 nanocomposite, Ceram Int., 49 (2023) 7. https://doi.org/10.1016/j.ceramint.2022.11.298.
8. X.L Li, S, Raza, C. Liu, Directly electrospinning synthesized Z-scheme heterojunction TiO_2@Ag@Cu_2O nanofibers with enhanced photocatalytic degradation activity under solar light irradiation, J Environ Eng, 9 (2021) 106133, https://doi.org/10.1016/j.jece.2021.106133.
9. B., Azari, A., Pourahmad, B., Sadeghi, M., Mokhtary, Green synthesis of SiO_2 from Equisetnm arvense plant for synthesis of SiO_2/ZIF-8 MOF nanocomposite as photocatalyst, J Coord Chem., 321 (2023) 219-231, https://doi.org/10.1080/00958972.2023.2166408.
10. K.S. Min, R.S. Kumar, J.H. Lee, K.S. Kim, S.G. Lee, Y.A. Son, Synthesis of new TiO_2/porphyrin-based composites and photocatalytic studies on methylene blue degradation, Dyes and Pigments, 160 (2019) 37-47, https://doi.org/10.1016/j.dyepig.2018.07.045.
11. B.H., Yao, C., Peng, W., Zhang, Q. J., Zhang, F. J., Zhao, A novel Fe(III) porphyrin-conjugated TiO_2 visible-light photocatalyst, Appl Catal B-Environ, 174-175 (2015) 77-84, https://doi.org/10.1016/j.apcatb.2015.02.030.